# $^{129}$Xe-$^{128}$Xe and $^{40}$Ar-$^{39}$Ar CHRONOLOGY OF TWO ANTARCTIC ENSTATITE METEORITES

Masahiko HONDA, Thomas J. BERNATOWICZ and FRANK A. PODOSEK

*McDonnell Center for the Space Sciences, Washington University, St. Louis, Missouri 63130, U.S.A.*

***Abstract:*** $^{129}$Xe-$^{128}$Xe and $^{40}$Ar-$^{39}$Ar analyses have been performed on two Antarctic enstatite meteorites, the chondrite Y-691 and the aubrite (enstatite achondrite) ALH-78113. Both meteorites have complex $^{40}$Ar-$^{39}$Ar release patterns to which no unambiguous age assignment is possible. Both give apparently satisfactory $^{129}$Xe-$^{128}$Xe correlations corresponding to unusual ages. The I-Xe age of the chondrite Y-691 is 16 Ma after Bjurbole, not unusual for chondrites in general but 10 Ma later than previously known ages for enstatite chondrites. The I-Xe age of the aubrite ALH-78113 is 210 Ma after Bjurbole, the latest age (rather than a limit) so far observed by the I-Xe technique, but this age assignment must be considered tentative because of the possibility that it is significantly influenced by terrestrial I contamination.

## 1. Introduction

The decay of the natural radionuclides $^{129}$I and $^{40}$K to noble gas daughters $^{129}$Xe and $^{40}$Ar, respectively, provides the basis for two geochronological methodologies which are widely applicable to the study of the history of meteorites. We report here the results of applying these methods to two meteorites recovered from Antarctica, Y-691 and ALH-78113. In both geochronological methods we have employed the approach in which neutron irradiation is used to produce another noble gas isotope ($^{128}$Xe and $^{39}$Ar) from another isotope of the parent ($^{127}$I and $^{39}$K) element to serve as a tracer for the parent isotope and in which gas is released in stepwise heating to investigate and compensate for partial loss of the radiogenic daughter.

Both samples studied are enstatite meteorites. This is a relatively rare class of meteorites, including both chondrites and achondrites, whose principal geochemical characteristic is an extreme degree of reduction. Previous I-Xe studies have shown that, in contrast to chondrites in general, enstatite chondrite ages cluster closely, falling into two groups according to petrologic classification (*cf.* KENNEDY and PODOSEK, 1978; KENNEDY, 1981); there are only a few ages for the achondrites, and generalizations such as this have not emerged. This work was undertaken to extend the data base for this interesting class of meteorites and study age relationships within the class.

## 2. Samples

Y-691 is an enstatite chondrite, composed primarily of clinoenstatite, enstatite and opaque minerals, with small amounts of olivine, plagioclase, cristobalite and glass

(OKADA, 1975; OKADA *et al.*, 1975). OKADA *et al.* suggest that it is an unmetamorphosed chondrite, type E4 in the classification of VAN SCHMUS and WOOD (1967) or Type I in that of KEIL (1968); CRABB and ANDERS (1981) list it E4 or E5 (Type I or intermediate between Types I and II).

ALH-78113 is an aubrite (enstatite achondrite) for which only scant petrographic information is available. It consists of large clasts of orthopyroxene in a groundmass of comminuted pyroxene with accessory sulfide and metal grains (MASON, 1981).

Samples of both meteorites were obtained from the National Institute of Polar Research (Japan). Approximately one gram of each was broken into chips up to a few mm diameter. Both samples are extensively weathered. Those pieces which were obviously weathered (in binocular microscope observation) were removed from the specimens which were subsequently irradiated. The unirradiated sample of ALH-78113 consisted of the weathered pieces removed from the irradiated sample.

## 3. Experimental Procedures

### *3.1. Neutron irradiation*

All samples and monitors were wrapped in Al foil and sealed in quartz vials under rough vacuum ($10^{-2}$ torr). The vials were loaded in a can and irradiated in the rotating can facility at the graphite reflector position in the Research Reactor Facility, University of Missouri (Columbia). This irradiation (March 1982, Laboratory designation SLC-7) was for 80 hours at a nominal thermal neutron flux of $3.5\times10^{13}$cm$^{-2}$s$^{-1}$.

The primary monitor for the $^{127}$I $(n, \gamma\beta)$ $^{128}$Xe reaction was the meteorite Bjurbole. The primary monitor for the $^{39}$K $(n,p)$ $^{39}$Ar reaction was the terrestrial hornblende hb3gr. Other neutron reactions were monitored by samples of $CaF_2$ and $K_2SO_4$. Analysis of monitors as well as samples is described below and the results summarized in Table 1.

*Table 1. Irradiation parameters for SLC-7*[a].

| Integrated flux (80 hr) | | $1.32\times10^{19}$ n/cm$^2$ |
|---|---|---|
| Ca production | $^{37}$Ar/Ca | $7.74\times10^{-6}$ |
| | $^{36}$Ar/$^{37}$Ar | $(2.13\pm0.04)\times10^{-4}$ |
| | $^{38}$Ar/$^{37}$Ar[b] | $(1.0\ \pm0.5\ )\times10^{-4}$ |
| | $^{39}$Ar/$^{37}$Ar | $(1.02\pm0.03)\times10^{-3}$ |
| K production | $^{39}$Ar/K | $2.94\times10^{-5}$ |
| | $^{38}$Ar/$^{39}$Ar | $(1.71\pm0.02)\times10^{-2}$ |
| | $^{40}$Ar/$^{39}$Ar | $(1.34\pm0.01)\times10^{-1}$ |
| Cl production | $^{38}$Ar/Cl[c] | $8.39\times10^{-4}$ |
| | $^{36}$Ar/$^{38}$Ar[d] | $(4.3\ \pm1.3\ )\times10^{-4}$ |
| I production | $^{128}$Xe/I | $(1.30\pm0.06)\times10^{-2}$ |

a) Absolute production rates are units of cm$^3$STP/g target, relative production rates are atomic ratio.
b) Adopted from TURNER *et al.* (1978).
c) Absolute production rate was calculated from the $^{37}$Cl thermal neutron capture cross section (0.433 barns) and estimated thermal neutron fluence from Bjurbole (see text).
d) Calculated following BERNATOWICZ *et al.* (1978).

Each vial contained flux wires to monitor spatial variations in neutron fluence within the irradiation can. Thermal neutron variations were monitored by counting $^{60}$Co activities produced by $^{59}$Co $(n, \gamma)$ in Co-doped Al wires and fast neutron variations were monitored by counting $^{58}$Co produced by $^{58}$Ni $(n, p)$ in Ni wires. Total variations in thermal and fast fluence were less than 3% and 4%, respectively. All the values in Table 1 are adjusted to the fluence at the position of Bjurbole.

### 3.2. *Mass spectrometry*

Samples in the same Al foil wrappers in which they were irradiated were analyzed by stepwise heating in a well-degassed Mo crucible heated by RF induction. Temperatures were calibrated by means of an optical pyrometer, to an estimated accuracy of $\pm 50$°C. After heating for one hour at each temperature, liberated gases were purified by a Ti-Zr bulk getter maintained at 800°C and a series of flash getters. Only Ar and Xe were analyzed. Ar and Xe were separated by adsorption of Xe on a charcoal cooled by a dry ice-acetone slurry (−81°C).

*Table 2. Xenon in neutron-irradiated meteorites (SLC-7)*[a].

| Temperature (°C) | [$^{132}$Xe] cm$^3$STP/g $\times 10^{-12}$ | ($^{132}$Xe=1.0) $^{124}$Xe | $^{126}$Xe | $^{128}$Xe | $^{129}$Xe | $^{130}$Xe | $^{131}$Xe | $^{134}$Xe | $^{136}$Xe |
|---|---|---|---|---|---|---|---|---|---|
| | | | | Bjurbole (L4) 0.5917g | | | | | |
| 600 | 1.6 | 0.00448 ±56 | 0.00503 ±58 | 20.969 ±1.750 | 1.182 ±24 | 0.1604 ±24 | 4.594 ±416 | 0.382 ±4 | 0.323 ±5 |
| 800 | 5.5 | 0.00341 ±14 | 0.00378 ±25 | 8.614 ±.326 | 0.842 ±9 | 0.0991 ±14 | 3.318 ±129 | 0.893 ±15 | 1.081 ±27 |
| 900 | 5.4 | 0.00493 ±34 | 0.00460 ±18 | 5.156 ±147 | 1.425 ±15 | 0.1473 ±25 | 2.933 ±88 | 0.581 ±7 | 0.628 ±10 |
| 1000 | 16.1 | 0.00465 ±8 | 0.00482 ±20 | 1.576 ±15 | 1.553 ±7 | 0.1609 ±12 | 1.513 ±10 | 0.411 ±4 | 0.361 ±5 |
| 1100 | 115.6 | 0.00484 ±8 | 0.00440 ±7 | 0.665 ±4 | 1.758 ±6 | 0.1621 ±6 | 1.012 ±2 | 0.387 ±2 | 0.330 ±3 |
| 1200 | 74.0 | 0.00480 ±12 | 0.00427 ±16 | 0.747 ±7 | 1.893 ±9 | 0.1638 ±6 | 0.949 ±4 | 0.386 ±2 | 0.328 ±3 |
| 1250 | 52.1 | 0.00449 ±11 | 0.00397 ±11 | 0.429 ±3 | 1.496 ±4 | 0.1611 ±9 | 0.880 ±3 | 0.388 ±2 | 0.331 ±3 |
| 1300 | 64.0 | 0.00479 ±14 | 0.00405 ±13 | 0.487 ±4 | 1.597 ±6 | 0.1632 ±6 | 0.906 ±3 | 0.384 ±3 | 0.323 ±3 |
| 1350 | 49.3 | 0.00474 ±11 | 0.00402 ±13 | 0.646 ±6 | 1.824 ±9 | 0.1625 ±9 | 1.018 ±4 | 0.391 ±3 | 0.334 ±3 |
| 1400 | 14.3 | 0.00464 ±17 | 0.00404 ±19 | 0.813 ±12 | 2.061 ±20 | 0.1596 ±9 | 1.556 ±19 | 0.400 ±3 | 0.349 ±4 |
| 1450 | 3.7 | 0.00446 ±27 | 0.00439 ±42 | 0.682 ±28 | 1.814 ±40 | 0.1571 ±19 | 5.054 ±308 | 0.398 ±4 | 0.346 ±6 |
| 1550 | 2.3 | 0.00430 ±11 | 0.00431 ±41 | 0.613 ±38 | 1.585 ±58 | 0.1548 ±25 | 11.709 ±1.071 | 0.413 ±5 | 0.372 ±6 |
| Total | 403.9 | 0.00473 ±4 | 0.00422 ±5 | 0.906 ±9 | 1.714 ±3 | 0.1612 ±3 | 1.173 ±7 | 0.398 ±1 | 0.346 ±1 |

a) Tabulated data have been corrected for instrumental discrimination, procedural blank and neutron-induced interferences (see text). Uncertainties are one standard deviation.

*Table 2. Continued.*

| Temperature (°C) | [$^{132}$Xe] cm$^3$STP/g $\times 10^{-12}$ | ($^{132}$Xe=1.0) $^{124}$Xe | $^{126}$Xe | $^{128}$Xe | $^{129}$Xe | $^{130}$Xe | $^{131}$Xe | $^{134}$Xe | $^{136}$Xe |
|---|---|---|---|---|---|---|---|---|---|
| | | Y-691 (E4 or 5) 0.9272g | | | | | | | |
| 500 | 44. | 0.00369 ±7 | 0.00306 ±8 | 8.761 ±47 | 1.024 ±3 | 0.1528 ±7 | 0.940 ±2 | 0.387 ±2 | 0.331 ±3 |
| 600 | 35. | 0.00364 ±8 | 0.00317 ±7 | 4.759 ±26 | 1.032 ±4 | 0.1534 ±6 | 0.903 ±2 | 0.389 ±2 | 0.332 ±3 |
| 700 | 86. | 0.00382 ±5 | 0.00347 ±6 | 3.440 ±17 | 1.040 ±2 | 0.1533 ±6 | 0.933 ±2 | 0.386 ±2 | 0.329 ±3 |
| 800 | 129. | 0.00381 ±7 | 0.00349 ±6 | 3.035 ±14 | 1.058 ±2 | 0.1542 ±5 | 1.045 ±2 | 0.389 ±2 | 0.331 ±3 |
| 900 | 170. | 0.00391 ±8 | 0.00354 ±6 | 5.631 ±25 | 1.206 ±3 | 0.1538 ±7 | 1.265 ±3 | 0.417 ±2 | 0.374 ±4 |
| 1000 | 443. | 0.00446 ±6 | 0.00394 ±5 | 2.666 ±12 | 1.775 ±4 | 0.1604 ±5 | 0.935 ±2 | 0.402 ±2 | 0.353 ±3 |
| 1050 | 181. | 0.00456 ±9 | 0.00403 ±8 | 2.479 ±11 | 2.494 ±5 | 0.1609 ±6 | 0.876 ±2 | 0.391 ±2 | 0.335 ±3 |
| 1100 | 147. | 0.00448 ±4 | 0.00401 ±9 | 1.380 ±6 | 1.765 ±4 | 0.1617 ±6 | 0.847 ±2 | 0.387 ±2 | 0.329 ±3 |
| 1200 | 199. | 0.00451 ±6 | 0.00407 ±6 | 0.971 ±5 | 1.530 ±4 | 0.1611 ±5 | 0.849 ±2 | 0.384 ±2 | 0.323 ±3 |
| 1250 | 121. | 0.00458 ±6 | 0.00408 ±9 | 1.045 ±5 | 1.607 ±4 | 0.1619 ±5 | 0.858 ±2 | 0.383 ±2 | 0.323 ±3 |
| 1300 | 83. | 0.00473 ±6 | 0.00417 ±9 | 1.471 ±9 | 1.956 ±12 | 0.1612 ±5 | 0.878 ±2 | 0.380 ±2 | 0.319 ±3 |
| 1350 | 158. | 0.00459 ±6 | 0.00409 ±6 | 1.324 ±7 | 1.836 ±4 | 0.1615 ±7 | 0.870 ±2 | 0.384 ±2 | 0.326 ±3 |
| 1400 | 88. | 0.00459 ±5 | 0.00414 ±6 | 0.773 ±4 | 1.428 ±3 | 0.1629 ±6 | 0.846 ±2 | 0.380 ±2 | 0.318 ±3 |
| 1450 | 47. | 0.00457 ±7 | 0.00396 ±8 | 0.718 ±3 | 1.374 ±3 | 0.1618 ±7 | 0.845 ±2 | 0.386 ±2 | 0.327 ±3 |
| 1500 | 11. | 0.00442 ±13 | 0.00400 ±17 | 0.884 ±6 | 1.393 ±6 | 0.1645 ±10 | 0.904 ±2 | 0.380 ±3 | 0.316 ±3 |
| 1550 | 16. | 0.00450 ±17 | 0.00364 ±10 | 0.869 ±5 | 1.381 ±4 | 0.1612 ±9 | 0.908 ±3 | 0.386 ±2 | 0.326 ±3 |
| 1600 | 1. | 0.00415 ±16 | 0.00397 ±42 | 0.883 ±29 | 1.341 ±14 | 0.1563 ±13 | 1.312 ±45 | 0.396 ±5 | 0.341 ±4 |
| Total | 1958. | 0.00436 ±2 | 0.00389 ±2 | 2.454 ±4 | 1.628 ±1 | 0.1594 ±2 | 0.931 ±1 | 0.392 ±1 | 0.337 ±1 |

Separate mass spectrometers were used for Ar and Xe analyses, one operated with electron multiplier and source magnet for Xe, the other without source magnet or multiplier (direct ion collection) for Ar. Both are Reynolds-type spectrometers (4.5 inch radius, 60° sector, single focusing). Methods of gas analysis and data reduction are described in detail by DROZD (1974). Instrumental sensitivity and isotopic mass discrimination were determined by repeated analysis of pipetted aliquots of air. Instrumental sensitivity variations of Ar and Xe were 2% and 5%, respectively, and absolute sensitivities are believed accurate within 20%. The basic experimental results are presented in Tables 2, 3 and 4.

*Table 2. Continued.*

| Temperature (°C) | [$^{132}$Xe] cm$^3$STP/g $\times 10^{-12}$ | ($^{132}$Xe=1.0) $^{124}$Xe[a] | $^{126}$Xe[a] | $^{128}$Xe | $^{129}$Xe | $^{130}$Xe | $^{131}$Xe | $^{134}$Xe | $^{136}$Xe |
|---|---|---|---|---|---|---|---|---|---|
| | | | ALH-78113 (Aubrite) 1.0704g | | | | | | |
| 500 | 3.2 | | | 1419. | 1.066 | 0.116 | 1.204 | 0.349 | 0.284 |
| | | | | ±35 | ±65 | ±8 | ±29 | ±13 | ±6 |
| 600 | 1.0 | | | 2854. | 1.184 | 0.172 | 2.194 | 0.362 | 0.303 |
| | | | | ±103 | ±12 | ±2 | ±138 | ±4 | ±5 |
| 700 | 0.9 | | | 2927. | 1.217 | 0.181 | 2.967 | 0.375 | 0.312 |
| | | | | ±124 | ±14 | ±3 | ±179 | ±4 | ±4 |
| 800 | 4.4 | | | 842. | 0.448 | 0.067 | 1.636 | 1.171 | 1.541 |
| | | | | ±13 | ±25 | ±3 | ±23 | ±19 | ±23 |
| 900 | 5.2 | | | 975. | 0.771 | 0.097 | 2.306 | 0.995 | 1.270 |
| | | | | ±17 | ±18 | ±3 | ±33 | ±10 | ±20 |
| 1000 | 1.9 | | | 967. | 1.336 | 0.150 | 2.728 | 0.479 | 0.474 |
| | | | | ±25 | ±16 | ±2 | ±136 | ±8 | ±12 |
| 1100 | 2.0 | | | 982. | 1.333 | 0.148 | 2.707 | 0.520 | 0.526 |
| | | | | ±22 | ±12 | ±1 | ±75 | ±11 | ±15 |
| 1200 | 1.9 | | | 690. | 1.302 | 0.150 | 1.845 | 0.485 | 0.458 |
| | | | | ±17 | ±12 | ±2 | ±55 | ±8 | ±10 |
| 1300 | 4.9 | | | 373. | 1.235 | 0.155 | 1.301 | 0.456 | 0.431 |
| | | | | ±8 | ±6 | ±1 | ±11 | ±5 | ±6 |
| 1400 | 4.2 | | | 188. | 1.187 | 0.158 | 1.092 | 0.416 | 0.360 |
| | | | | ±4 | ±5 | ±2 | ±5 | ±4 | ±5 |
| 1500 | 1.6 | | | 216. | 1.180 | 0.160 | 1.252 | 0.414 | 0.364 |
| | | | | ±6 | ±7 | ±1 | ±32 | ±3 | ±6 |
| 1600 | 1.2 | | | 228. | 1.210 | 0.153 | 1.576 | 0.432 | 0.394 |
| | | | | ±8 | ±11 | ±2 | ±44 | ±5 | ±6 |
| Total | 32.4 | | | 840. | 1.041 | 0.131 | 1.754 | 0.623 | 0.691 |
| | | | | ±7 | ±8 | ±1 | ±14 | ±4 | ±5 |

a) The amount of $^{128}$Xe required operation at sufficiently low electronic amplification that $^{124}$Xe and $^{126}$Xe were undetectable.

Procedural blanks using the sample procedure but without a sample in the crucible were taken before and between sample analyses. Isotopic compositions of procedural blanks were the same as those of air within experimental errors (except as noted below). Typical $^{40}$Ar blanks at 1200°C and 1500°C were 4.2 and 5.4 in units of $10^{-8}$cm$^3$ STP, respectively. The variation of Ar blanks repeatedly analyzed at 1200°C was within 30%. $^{132}$Xe blanks were essentially constant (within 15%) at $3\times10^{-13}$ cm$^3$ STP at any temperature. We assigned uncertainties to Ar and Xe blanks of 30% and 15%, respectively.

Because of the extremely high $^{128}$Xe levels and $^{128}$Xe/$^{130}$Xe ratios in ALH-78113 (Table 2), blanks run after ALH-78113 showed substantial excesses of $^{128}$Xe (relative to atmospheric composition). This did not affect Bjurbole or Y-691, which were analyzed before ALH-78113, but it did affect the analysis of unirradiated ALH-78113, which was analyzed after the irradiated sample. The $^{128}$Xe data for unirradiated ALH-78113 (Table 4) are thus not reliable.

*Table 3. Argon in neutron-irradiated meteorites (SLC-7)*[a].

| Temperature °C | [$^{40}$Ar] cm$^3$STP/g $\times 10^{-7}$ | ($^{40}$Ar=1.0) $^{36}$Ar | $^{37}$Ar[b,c] | $^{38}$Ar | $^{39}$Ar[b] | Apparent $^{40}$Ar-$^{39}$Ar age[d] (AE) |
|---|---|---|---|---|---|---|
| | | Y-691 (E4 or 5) 0.9272g | | | | |
| 500 | 1.1 | 0.0062± 2 | 0.094±161 | 0.0379±29 | 0.00290±23 | 1.66±11 |
| 600 | 0.7 | 0.0068± 4 | 0.190± 80 | 0.0458±47 | 0.00590±62 | 1.00± 8 |
| 700 | 1.5 | 0.0079± 3 | 0.288± 34 | 0.0538±34 | 0.00760±48 | 0.82± 3 |
| 800 | 2.6 | 0.0084± 2 | 0.053± 6 | 0.0608±25 | 0.00726±31 | 0.83± 3 |
| 900 | 6.7 | 0.0078± 1 | 0.050± 5 | 0.0407± 8 | 0.00340± 7 | 1.47± 2 |
| 1000 | 28.2 | 0.0104± 1 | 0.007± 2 | 0.0118± 1 | 0.00098± 3 | 3.02± 5 |
| 1050 | 9.6 | 0.0130± 1 | — | 0.0078± 1 | 0.00075± 3 | 3.43± 5 |
| 1100 | 1.7 | 0.0508± 31 | — | 0.0224±14 | 0.00261±17 | 1.74± 7 |
| 1200 | 1.2 | 0.0873± 72 | — | 0.0335±28 | 0.00330±29 | 1.49± 9 |
| 1250 | 0.9 | 0.0652± 65 | — | 0.0283±29 | 0.00276±29 | 1.68±12 |
| 1300 | 1.0 | 0.0380± 36 | — | 0.0222±22 | 0.00229±24 | 1.89±12 |
| 1350 | 1.9 | 0.0338± 20 | 0.048± 6 | 0.0212±14 | 0.00175±12 | 2.26± 9 |
| 1400 | 0.8 | 0.0546± 66 | — | 0.0238±30 | 0.00148±20 | 2.43±18 |
| 1450 | 0.2 | 0.1067±244 | — | 0.0394±92 | 0.00203±52 | 2.03±31 |
| Total | 58.1 | 0.0160± 3 | 0.025± 4 | 0.0204± 2 | 0.00195± 3 | 2.10± 2 |

*Table 3. Continued.*

| Temperature °C | [$^{40}$Ar] cm$^3$STP/g $\times 10^{-7}$ | ($^{40}$Ar=1.0) $^{36}$Ar | $^{37}$Ar | $^{38}$Ar | $^{39}$Ar | Apparent age (AE) |
|---|---|---|---|---|---|---|
| | | ALH-78113 (Aubrite) 1.0704g | | | | |
| 500 | 7.4 | 0.00165± 3 | — | 0.00348± 4 | 0.00042± 1 | 4.36± 5 |
| 600 | 7.9 | 0.00040± 4 | — | 0.00252± 3 | 0.00065± 1 | 3.63± 3 |
| 700 | 12.0 | 0.00024± 3 | — | 0.00135± 1 | 0.00052± 1 | 4.00± 2 |
| 800 | 15.5 | 0.00025± 2 | — | 0.00102± 1 | 0.00046± 1 | 4.18± 4 |
| 900 | 16.1 | 0.00040± 2 | — | 0.00131± 1 | 0.00046± 1 | 4.18± 3 |
| 1000 | 5.6 | 0.00066± 5 | — | 0.00169± 2 | 0.00078± 2 | 3.36± 3 |
| 1100 | 3.6 | 0.00123± 7 | — | 0.00258± 6 | 0.00146± 5 | 2.45± 4 |
| 1200 | 1.1 | 0.00393± 6 | — | 0.00763± 58 | 0.00313±26 | 1.54± 9 |
| 1300 | 1.6 | 0.00492±11 | — | 0.00796± 49 | 0.00210±14 | 1.99± 8 |
| 1400 | 0.8 | 0.00669±37 | — | 0.00973±103 | 0.00165±21 | 2.15±15 |
| 1500 | 0.4 | 0.00484±27 | — | 0.00839±138 | 0.00217±39 | 1.95±21 |
| 1600 | 0.2 | 0.00540±51 | — | 0.00919±196 | 0.00277±64 | 1.67±25 |
| Total | 72.1 | 0.00789±12 | — | 0.00209± 2 | 0.00067± 1 | 3.59± 2 |

a) Tabulated isotopic ratios have been corrected for instrumental mass discrimination, procedural blank and have been flux normalized to the Bjurbole irradiation position. Errors are one standard deviation.

b) $^{37}$Ar and $^{39}$Ar results have been corrected for decay ($\lambda 37 = 1.98\times10^{-2}$ day$^{-1}$ and $\lambda 39 = 7.06\times10^{-6}$ day$^{-1}$) during and since irradiation.

c) Some of $^{37}$Ar results were below detection limit ($\times 10^{-12}$ cm$^3$STP).

d) $^{40}$Ar-$^{39}$Ar age was calculated by using the following recommended values by STEIGER and JAGER (1977) for $^{40}$K; $\lambda\beta^- = 4.962\times10^{-10}$yr$^{-1}$, $\lambda = 0.581\times10^{-10}$yr$^{-1}$, $^{40}$K/K$=1.167\times10^{-4}$. Uncertainties of ages are based upon the errors of $^{40}$Ar*/$^{39}$Ar* ratios (see text).

### 3.3. *Irradiation monitors*

The L4 chondrite Bjurbole was used to monitor the conversion of $^{127}$I to $^{128}$Xe in

*Table 4. Xenon in unirradiated ALH-78113 (0.2427g)*[a].

| Temperature (°C) | [$^{132}$Xe] cm$^3$STP/g $\times 10^{-12}$ | ($^{132}$Xe=1.0) $^{124}$Xe | $^{126}$Xe | $^{128}$Xe[b] | $^{129}$Xe | $^{130}$Xe | $^{131}$Xe | $^{134}$Xe | $^{136}$Xe |
|---|---|---|---|---|---|---|---|---|---|
| 600 | 4.4 | 0.00406 ±51 | 0.00384 ±47 | 0.068 ±163 | 1.042 ±9 | 0.1516 ±23 | 0.333 ±83 | 0.381 ±5 | 0.320 ±7 |
| 1500 | 14.6 | 0.00573 ±23 | 0.00552 ±28 | — | 1.344 ±14 | 0.1574 ±12 | 0.680 ±25 | 0.390 ±3 | 0.334 ±5 |
| Total | 19.0 | 0.00534 ±21 | 0.00513 ±24 | — | 1.274 ±11 | 0.1561 ±11 | 0.600 ±27 | 0.387 ±3 | 0.331 ±4 |

a) Errors are one standard deviation.
b) $^{128}$Xe data are unreliable because of high $^{128}$Xe in preceding blanks (see text).

the neutron irradiation (*cf.* PODOSEK, 1970). Gas analysis and data handling for Xe were the same as for the Antarctic meteorite samples, but Ar was not analyzed. Xe data are included in Table 2. The high-temperature data yield a well-defined correlation (Fig. 1) between $^{128}$Xe and $^{129}$Xe with a slope of $1.48 \pm 0.05$ (Table 6); this slope is the ratio of $^{129}$Xe* (produced by decay of $^{129}$I) to $^{128}$Xe* (produced in the irradiation) in the most retentive sites. Assuming this corresponds to $^{129}I/^{127}I = 1.095 \times 10^{-4}$ (HOHENBERG and KENNEDY, 1981), the efficiency of $^{128}$Xe* production is given by $^{128}Xe^*/^{127}I = 1.30 \times 10^{-2}$ cm$^3$ STP/g (Table 1). For an assumed thermal neutron cross section of 6.1 barns, the corresponding fluence is $1.32 \times 10^{19}$ neutrons/cm$^2$. This is probably an overestimate of thermal fluence because a significant fraction of the $^{128}$Xe* is likely produced by epithermal resonance capture by $^{127}$I (*cf.* HUDSON *et al.*, 1983). It should be noted, however, that the absolute values of both the fluence and the $^{128}Xe^*/^{127}I$ con-

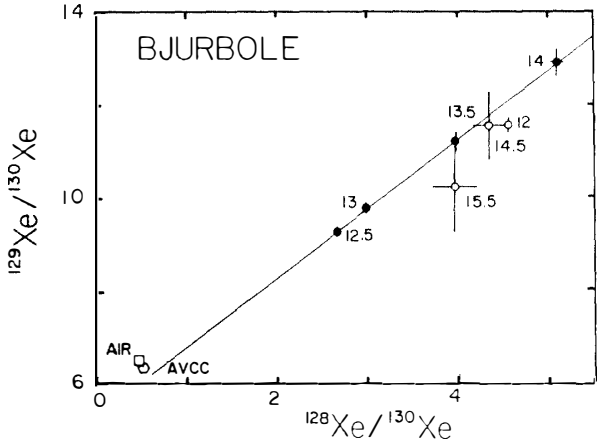


*Fig. 1. I-Xe correlation diagram for the Bjurbole I-Xe standard. Data are corrected for all contributions other than trapped and iodine-derived Xe. Data points are labeled according to extraction temperature in 100° C. The solid line is a least squares fit (Table 6) to the solid data points (1250–1400° C). Error limits illustrated are one standard deviation.*

version efficiencies are irrelevant to the chronological comparison of the Antarctic meterorites with Bjurbole, since this comparison rests on the ratios of correlation slopes (PODOSEK, 1970). The I concentrations (Table 6) are based on the tabulated value of $^{128}Xe^*/^{127}I$ but do not involve the nominal neutron fluence.

The principal irradiation parameter necessary for $^{40}Ar$-$^{39}Ar$ analysis is the efficiency of the $^{39}K(n, p)$ reaction, determined as $^{39}Ar^*/K$ (Table 1) by analysis of $^{39}Ar^*/^{40}Ar^*$ in hb3gr included in the irradiation and the value $^{40}Ar^*/K=(5.69\pm0.09)\times10^{-3}$ cm$^3$ STP/g measured by TURNER *et al.* (1971). ($^{39}Ar^*$ is that produced by $^{39}K(n, p)$, $^{40}Ar^*$ is that produced by decay of $^{40}K$). SLC-7 included 3 samples of hb3gr (H1–3). Gas from H2 was inexplicably lost. Monitor H3, which yielded $[^{40}Ar^*]=5.5\times10^{-5}$cm$^3$ STP/g (TURNER *et al.* (1971) obtained $7.1\times10^{-5}$ cm$^3$ STP/g) and $^{39}Ar^*/^{40}Ar^*=(5.22\pm0.07)\times10^{-3}$, is the basis for the $^{39}Ar^*/K=2.94\times10^{-5}$ cm$^3$ STP/g cited in Table 1. H1 gave $[^{40}Ar^*]=3.6\times10^{-5}$ cm$^3$ STP/g and $^{39}Ar^*/^{40}Ar^*=(5.92\pm0.09)\times10^{-3}$. This $^{39}Ar^*/^{40}Ar^*$ ratio is 13% higher than the H3 value, well outside either the stated precision or the range of variation noted by TURNER *et al.* We do not understand the discrepancy, and have adopted the H3 datum for normalization on the grounds that if the lower $[^{40}Ar^*]$ in H1 reflects gas loss either in irradiation or analysis the loss might also have introduced an isotopic variation. Adoption of H1 rather than H3 would produce apparent $^{40}Ar$-$^{39}Ar$ meteorite ages about 150 Ma higher than those based on H3. The $^{39}Ar^*/K$ from H3 is also the basis for the K concentrations in Table 5.

Production of $^{36}Ar$, $^{37}Ar$ and $^{39}Ar$ from irradiation of Ca was determined by analysis of the $CaF_2$ monitor. These data are given as $^{37}Ar/Ca$, $^{36}Ar/^{37}Ar$ and $^{39}Ar/^{37}Ar$ in Table 1. This $^{37}Ar/Ca$ value was used for calculation of Ca contents (Table 5) and the $^{36}Ar/^{37}Ar$ and $^{39}Ar/^{37}Ar$ ratios used for correction of interferences (see below). Direct detection of Ca-produced $^{38}Ar$ was impossible because of Cl contamination in the $CaF_2$, and the value in Table 1 is adopted from TURNER *et al.* (1978).

Analysis of the $K_2SO_4$ monitor was used to determine the production of $^{38}Ar$ and $^{40}Ar$ from K, cited as ratios to $^{39}Ar$ in Table 1. (As described above, the $^{39}Ar^*/K$ parameter is based on the hb3gr and not the $K_2SO_4$ monitor.)

No direct determination of Ar production from Cl was made. In Table 1, $^{38}Ar/Cl$ was estimated from the nominal thermal fluence based on $^{127}I$ capture and a $^{37}Cl$ capture cross section of 0.433 barns and a $^{36}Ar/^{38}Ar$ ratio calculated following BERNATOWICZ *et al.* (1978) (the tabulated value of $^{36}Ar/^{38}Ar$ is for 12 months after irradiation).

### *3.4. Xe component resolution*

The immediate objective in the Xe data analysis is identification of the I-derived components $^{129}Xe^*$ and $^{128}Xe^*$. The procedures followed are straightforward; they have most recently been described in detail by KENNEDY (1981), and the actual computational algorithms are given by HUDSON (1981).

After correction of the data for instrumental isotopic discrimination and subtraction of blanks, corrections were applied to $^{130}Xe$ for contributions from $^{129}Xe$ $(n,\gamma)$, to $^{132}Xe$ from $^{131}Xe$ $(n, \gamma)$, and to $^{126}Xe$ from $^{127}I$ $(n, 2n\beta)$. The data in Table 2 reflect this stage of analysis. In practice, for the present samples the "irradiation-interference" corrections are quite small (less than statistical errors) and the correction procedure essentially a formality.

Spallation Xe is identified on the basis of the $^{126}$Xe/$^{130}$Xe ratio, and corrections applied assuming (La+Ce+Nd)/Ba=0.52 (*cf.* HOHENBERG *et al.*, 1981a). As is evident from Table 2, spallation contributions are quite small in both Bjurbole and Y-691, and spallation corrections are again mostly a formality for these two meteorites. As noted in Table 2, we did not obtain $^{124}$Xe and $^{126}$Xe data for irradiated ALH-78113, so no spallation corrections were made in this case. Table 4, however, shows that spallation Xe is quite minor in ALH-78113 as well (formal resolution and target element concentrations from SHIMIZU and MASUDA (1981) indicate an exposure age less than about 5 Ma), so the absence of spallation corrections for the irradiated sample is unimportant.

At this stage in the procedure it is believed that $^{130}$Xe is all trapped and that $^{128}$Xe and $^{129}$Xe are mixtures of trapped and I-derived gas. These are the data shown in Figs. 1, 4 and 5, in which isotopic correlation is invoked to separate the trapped and I-derived components.

The remaining Xe component of customary interest is fission Xe, expected to be a mixture of $^{244}$Pu (and $^{238}$U) spontaneous fission and $^{235}$U neutron fission. In practice (for these samples) the significant fission component evidenced by elevated $^{134}$Xe and $^{136}$Xe, primarily around the 800°C fractions in Bjurbole and ALH-78113, is believed to be mostly $^{235}$U fission in the Al foil wrappers rather than in the samples themselves (*cf.* HOHENBERG *et al.*, 1981b). Fission Xe released from ALH-78113 from 1000°C and up, assuming AVCC trapped composition, is consistent with about 3 ppb U and/or 0.1 ppb $^{244}$Pu. Fission Xe in the Y-691 data is quite inconspicuous because of the large amounts of trapped Xe.

### *3.5. Ar component resolution*

In analogy to the case for Xe, the principal objective of Ar component analysis is identification of the K-derived components $^{40}$Ar* and $^{39}$Ar*. Detailed description of the procedures and computational algorithms is given by KENNEDY (1981) and HUDSON (1981).

The tabulation in Table 3 reflects correction for instrumental isotopic discrimination, blank subtraction, and correction of $^{37}$Ar and $^{39}$Ar for both decay after irradiation and spatial variations in neutron fluence.

All $^{37}$Ar is assumed to have been produced from Ca (Table 1), and $^{37}$Ar is accordingly used for calculation of Ca abundances (Table 5) and for correction of $^{36}$Ar, $^{38}$Ar and $^{39}$Ar for production from Ca. The remaining $^{39}$Ar is assumed to be all $^{39}$Ar*, *i.e.* derived from K, and is used for calculation of K contents (Table 5) and for correcting $^{38}$Ar and $^{40}$Ar for production from K (Table 1). The remaining $^{40}$Ar is taken to be $^{40}$Ar* (see below).

The remaining $^{36}$Ar and $^{38}$Ar are mixtures of trapped, spallation and Cl-derived components. Since there are more components than isotopes, formal resolution is impossible, and we have not attempted to separate these components. None of these components contains a large amount of either $^{39}$Ar or $^{40}$Ar, and the levels of $^{36}$Ar and $^{38}$Ar are low (Table 3), so we applied no further corrections to $^{39}$Ar and $^{40}$Ar. A possible fourth component contributing to $^{36}$Ar (and $^{38}$Ar) is atmospheric contamination. Since it is impossible to resolve an atmospheric contribution to $^{36}$Ar, no formal cor-

rection for atmospheric $^{40}Ar$ was applied.

For each release fraction the ratio of $^{40}Ar^*$ to $^{39}Ar^*$ corresponds to a $^{40}Ar^*/^{40}K$ ratio and thus to an age. The "apparent age" of each fraction is included in Table 3. The "apparent age" corresponding to total rock $^{40}Ar^*/^{39}Ar^*$, equivalent to the conventional K-Ar age, is also included in Table 5.

The analyses were not performed until approximately a year after the irradiation, when $^{37}Ar$ had decayed to the point of being undetectable in some of the Y-691 and all of the ALH-78113 release fractions (Table 3). The Ca contents in Table 5 are thus only limits. The Ca content of Y-691 is a lower limit, based only on those fractions in which $^{37}Ar$ was actually observed. For ALH-78113 the tabulated value is an upper limit, corresponding to the assumption that our detection limit ($\sim 10^{-12}$ cm$^3$ STP of $^{37}Ar$) was actually present in each fraction.

For our present purposes the absence of $^{37}Ar$ data is significant only in that without $^{37}Ar$ no correction for Ca-derived $^{39}Ar$ is possible. This is unlikely to be important for these samples, however. For scale, the data in Table 1 indicate that in a rock containing 1% Ca production of $^{39}Ar$ from Ca will be $7.9\times10^{-11}$cm$^3$ STP/g. For ALH-78113 the observed $^{39}Ar$ is $4.8\times10^{-9}$cm$^3$ STP/g, so 1% Ca would account for only 1.6 % of the observed $^{39}Ar$. The actual Ca concentration in ALH-78113 is probably significantly lower, *e.g.* if we take [K]=0.016% (Table 5) and an average aubrite Ca/K= 25 (WATTERS and PRINZ, 1979) the predicted Ca is 0.4% and the corresponding Ca contribution to $^{39}Ar$ only 0.7% of observed $^{39}Ar$. For Y-691 observed $^{39}Ar$ is $1.1\times10^{-8}$ cm$^3$ STP/g, so even 2% Ca would account for only 1.4% of observed $^{39}Ar$.

## 4. $^{40}Ar$-$^{39}Ar$ Chronology

The customary display of apparent age as a function of cumulative $^{39}Ar$ release for the two Antarctic meteorites is presented in Figs. 2 and 3. The canonical interpretation of such diagrams is that if apparent ages show a monotonically increasing trend with release fraction, reaching a "plateau" of constant ages over several fractions and a significant part of the total release, the plateau age can be identified with a real isotopic closure event in the history of that sample. It is evident from Figs. 2 and 3 that such a simple interpretation cannot be made for either meteorite.

Y-691 shows no plateau (Fig. 2), but rather a pattern of increasing apparent age over most of the release followed by a sharp decrease in the last 20%. Such a "high-temperature dropoff" is frequently observed and usually interpreted as artifact due to redistribution in the recoil of $^{39}Ar$ (*cf.* HUNEKE and SMITH, 1976). If so, the only chronological information to be obtained from Fig. 2 is that Y-691 first began to retain radiogenic $^{40}Ar$ more than 3.4 AE ago, but has since then experienced major loss of $^{40}Ar$, continuing to or at a time less than about 800 Ma ago (the 700°C and 800°C fractions).

The pattern for Y-691 (Fig. 2) is rather similar to that obtained for the intermediate-type E chondrite St. Sauveur by KENNEDY (1981). The whole-rock K-Ar age (Table 5) is similar to the 1.6 AE K-Ar age obtained by SHIMA *et al.* (1973) and the 1.4 AE U, Th-He age of CRABB and ANDERS (1981). The near concordance of K-Ar and U, Th-He ages led CRABB and ANDERS to suggest that Y-691 was nearly completely degas-

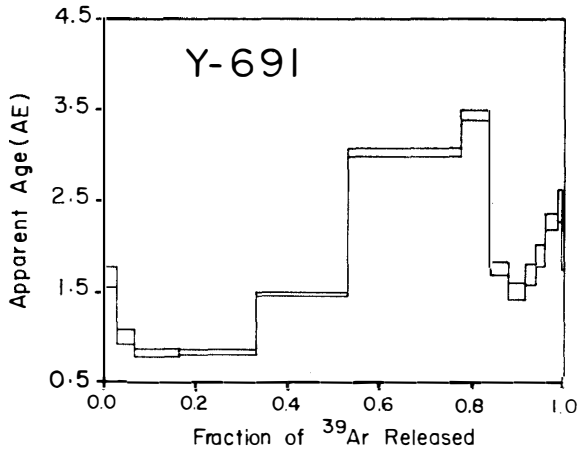


*Fig. 2.* *$^{40}Ar^*$-$^{39}Ar^*$ apparent ages as a function of cumulative $^{39}Ar^*$ release for Y-691. Apparent ages are plotted with one standard deviation errors based only on the uncertainties in $^{40}Ar^*/^{39}Ar^*$ ratios.*

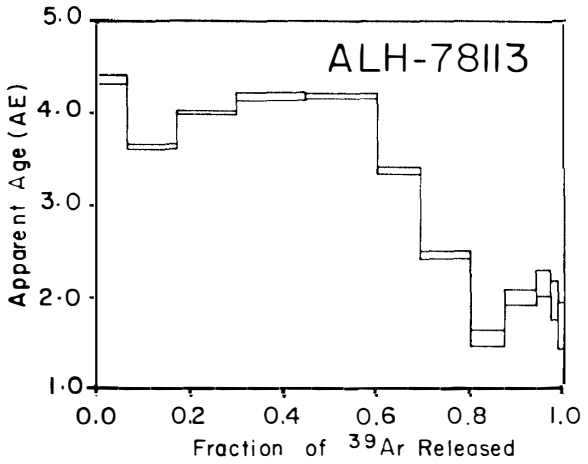


*Fig. 3.* *$^{40}Ar^*$-$^{39}Ar^*$ apparent ages for ALH-78113 (cf. Fig. 2).*

*Table 5. Summary of $^{40}Ar$-$^{39}Ar$ results.*

| Sample | (K) (wt %) | (Ca) (wt %) | $^{36}Ar$ ($\times 10^{-8}cm^3STP/g$) | K-Ar age (AE) |
|---|---|---|---|---|
| Y-691 | 0.039 | 1.88 | 9.30 | 2.10±0.02 |
| ALH-78113 | 0.016 | <0.4 | 5.69 | 3.59±0.02 |

sed around 1.5 AE ago (and has retained gases quantitatively since then) but this suggestion is obviously contradicted by Fig. 2.

$^{40}Ar$ loss from ALH-78113 has been less severe but the release pattern (Fig. 3) is nevertheless quite complicated. The high age for the first (500°C) fraction is presumably some sort of redistribution effect (or atmospheric contamination), as is the pattern of decreasing age in the last 40% of the release. If this "high-temperature drop-off" is a recoil effect it is unusually broad and deep. (Qualitatively, the same effect

could be accounted for by our failure to correct for Ca-produced $^{39}Ar$, but as noted earlier it appears quite unlikely that this is quantitatively important). If this is indeed redistribution by recoil, the release pattern suggests retention of $^{40}Ar$ began at least 4.2 AE ago (the age of the 800°C and 900°C fractions together accounting for about 30% of the $^{39}Ar$). In view of the Xe results for ALH-78113 it is tempting to attach the further significance of a real closure event at 4.2 AE (4.4 if we use the H1 monitor instead of H3), but this would be a very tenuous interpretation and hardly supportable from the Ar data alone.

## 5. $^{129}Xe$-$^{128}Xe$ Chronology

After the component resolution procedure described above has reached the point where the $^{128}Xe$-$^{129}Xe$-$^{130}Xe$ system is believed composed of only two components, trapped and I-derived, the I-derived component can in principle be determined by isotopic correlation as illustrated in Figs. 1, 4 and 5. Since there is no $^{130}Xe$ in the I component, the correlation slope is $^{129}Xe^*/^{128}Xe^*$, and by means of comparison with the slope of Bjurbole (PODOSEK, 1970), the age of a sample, relative to the age of Bjurbole, can be determined. The "age" is the time of Xe retention; more specifically the experiment measures the $^{129}I/^{127}I$ ratio at the time of Xe retention, and the age assignment requires the further assumption of isotopic homogeneity, *e.g.* that at any given time all samples had the same $^{129}I/^{127}I$. The value of $^{129}Xe/^{130}Xe$ at the time of isotopic closure is the value of the correlation at the trapped value of $^{128}Xe/^{130}Xe$; the trapped $^{129}Xe/^{130}Xe$ ratio is expected to be variable because of the growth of $^{129}Xe$ due to decay of $^{129}I$ before closure.

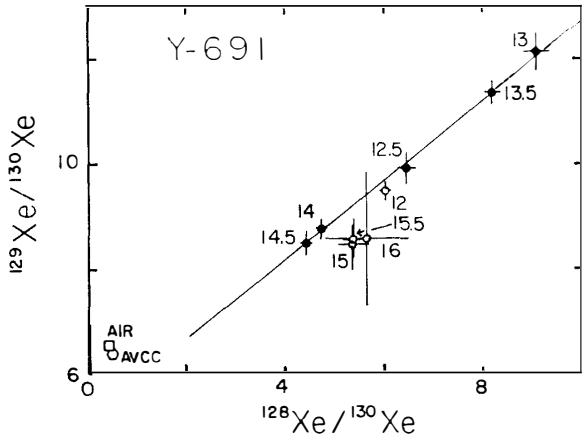


*Fig. 4. I–Xe correlation diagram for Y-691 (cf. Fig. 1). The 1250–1450° C extractions were used for the least squares fit (Table 6).*

In practice, not all data define a linear correlation as described above. Typically, only "high-temperature" (usually around 1100°C and higher) release fractions correlate linearly, with lower temperature data deviating in the direction of $^{129}Xe$ deficiency. This is usually interpreted as reflecting release from sites less retentive than those

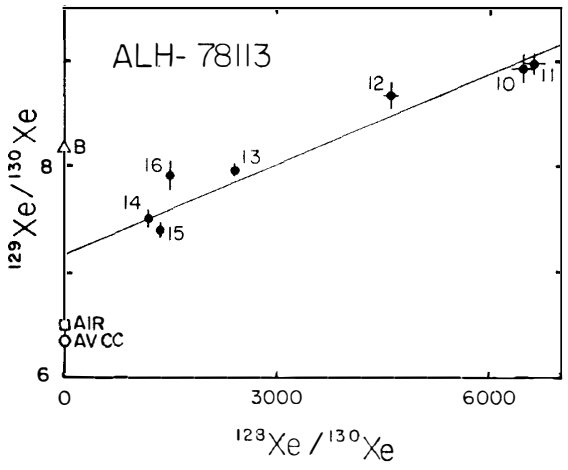


*Fig. 5. I–Xe correlation diagram for ALH-78113 (cf. Fig. 1). The 1000–1600°C extractions were used for the least squares fit (Table 6). On this scale the correlation line for Bjurbole is indistinguishable from the ordinate axis. The point B indicates the composition of unirradiated ALH-78113.*

making up the high-temperature correlation because of loss of $^{129}$Xe* after the high-temperature closure, perhaps very shortly after but also perhaps much later. Chronological interpretations are thus usually confined to the high-temperature correlation.

As is the general rule for enstatite chondrites, Y-691 exhibits a convincing high-temperature correlation (Fig. 4). Adjusted for fluence variation, the corresponding time of isotopic closure is 16 Ma after Bjurbole (Table 6). This age is not especially unusual for chondrites in general, but it is substantially later than ages previously found for enstatite chondrites. Previous ages have been relatively tightly clustered (PODOSEK, 1970; KENNEDY and PODOSEK, 1978; KENNEDY, 1981) at around 1 Ma before Bjurbole for E4 (Type I) chondrites and around 3 Ma after Bjurbole for E6 (Type II) chondrites. The previous latest age for enstatite chondrites is around 5 Ma after Bjurbole for the E5 (intermediate) chondrite St. Marks (PODOSEK, 1970). St. Marks has a rather high trapped $^{129}$Xe/$^{130}$Xe, suggesting that its age represents (nearly) closed system metamorphism. It is noteworthy that in Y-691 the later age is *not* accompanied by corresponding elevation of trapped $^{129}$Xe/$^{130}$Xe. It is not clear whether the age of Y-691 reflects metamorphism, shock or some other type of disturbance. If shock, caution in age interpretation is warranted, since the effects of shock on I-Xe systematics are not well understood (*cf.* CAFFEE *et al.*, 1982). Further caution is warranted since the effects of the extensive terrestrial residence and weathering characteristic of Antarctic meteorites are also unknown.

The correlation diagram for ALH-78113 is shown in Fig. 5. While there is scatter, subjectively the correlation appears real, particularly when it is noted that the uncertainties illustrated are only one standard deviation. The slope is very low and corresponds to "formation" 210 Ma after Bjurbole (Table 6). So great an age difference has never been measured previously by the I-Xe technique, and this result accordingly requires more careful consideration, particularly in view of other unusual features of

*Table 6. Summary of I-Xe dating.*

| Sample | Correlated temp. (°C) | Slope ($^{129}Xe^*/^{128}Xe^*$) | $\sqrt{\chi^2(N-2)}$ | $^{129}I/^{127}I$ $\times 10^{-4}$ | $\Delta t^{a)}$ ($10^6$ yr) | $^{129}Xe/^{130}Xe$ trapped | I (ppb) |
|---|---|---|---|---|---|---|---|
| Bjurbole | 1250–1400 | 1.484 ±.054 | 0.224 | 1.095[b] ±.029 | =.0 | 6.085 ±.052 | 31.6 |
| Y-691 | 1250–1450 | 0.757 ±.012 | 1.634 | 0.559 ±.027 | −16.5 ±1.0 | 5.695 ±.072 | 441. |
| ALH-78113 | 1000–1600 | 2.87 ±.19 $\times 10^{-4}$ | 1.749 | 2.12 ±.17 $\times 10^{-4}$ | −210. ±16. | 7.162 ±.061 | 2580. |

a) Ages calculated relative to Bjurbole (negative values indicate later formation).
b) From HOHENBERG and KENNEDY (1981).

the ALH-78113 Xe results.

The most obvious unusual feature is the extremely high I content (Table 6) and consequent domination of the measured Xe spectrum by $^{128}Xe^*$. The obvious inference is that so high an I concentration (most meteorites are in the range 10–100 ppb) represents terrestrial contamination rather than intrinsic meteoritic I, particularly since this is an Antarctic meteorite with a long terrestrial residence time. It is nevertheless possible to cite contrary evidence, however. One line of evidence is the release pattern for $^{128}Xe^*$ (Fig. 6), which is not confined to or even peaked at low temperatures. This is not conclusive but it is certainly suggestive that the I is indeed bound within mineral lattices rather than merely superficially sited; moreover the peak at 900°C (Fig. 6) is suggestive of release from troilite, a reasonable prospective host for I (*cf.* NIEMEYER, 1979). Another line of evidence is the correlation between $^{129}Xe^*$ and $^{128}Xe^*$ itself (Fig. 5), which seems real and which would have to be ascribed to coincidence if the $^{129}Xe^*$ and $^{128}Xe^*$ had separate origins and were not in the same locations in the meteorite (*e.g.* note in Fig. 6 that the release patterns of $^{128}Xe^*$ and $^{130}Xe$ are quite different).

Dominance of the Xe spectrum by $^{128}Xe$ is sufficiently great that we must also consider the possibility of artifacts. We have attempted to evaluate the possibility of two "artifacts" which are not usually considered but which might be significant in this extreme case.

One possibility is that the apparent $^{129}Xe^*$ is not actually real but is merely a scattering "tail" from the large $^{128}Xe$ peak. It should be noted that any such excess signal at mass 129 would be proportional to the signal at 128 and would produce an apparent linear correlation. We have investigated this possibility by examining "tailing" at the high-mass Xe isotopes at which there is no isotope one amu higher. There is no evident high-mass tailing above the level of about 1 part in $10^5$, and since the apparent correlation slope is $3 \times 10^{-4}$ (Table 6), this potential artifact appears quantitatively insufficient to account for the observations.

A second possible artifact is that the elevated signal really represents excess $^{129}Xe$ but that this excess still owes its origin to high $^{128}Xe$ because of neutron capture in the irradiation. This would also produce excess $^{129}Xe$ in proportion to $^{128}Xe$ and so lead

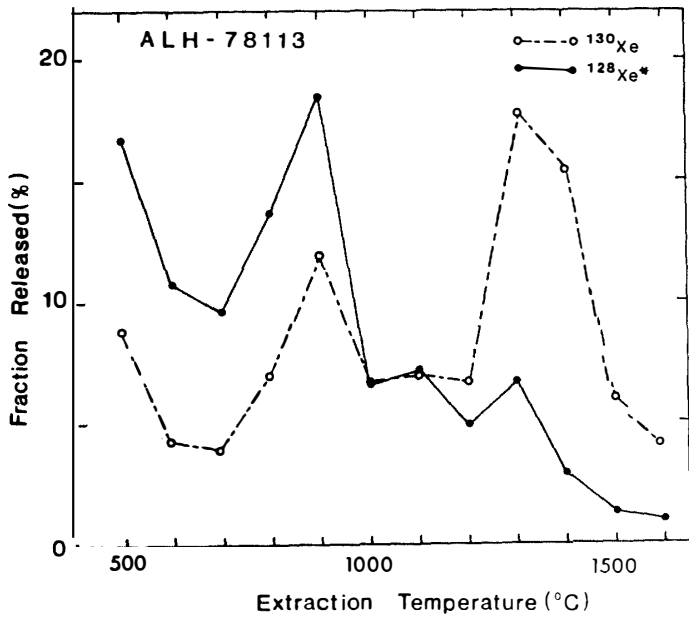


*Fig. 6. Fractional release diagram of $^{128}Xe^*$ and $^{130}Xe$ for ALH-78113. The maximum release in $^{130}Xe$ occurred at 1300°C, while that for $^{128}Xe^*$ occurred at 900°C indicating that iodine-induced $^{128}Xe$ and trapped $^{130}Xe$ occupy different sites.*

to an apparent correlation. This effect would produce a ratio of excess $^{129}Xe/^{128}Xe = 1/2\sigma\phi$, where $\phi$ is the neutron fluence and $\sigma$ is the cross section for $^{128}Xe$ $(n,\gamma)$ (the factor of 1/2 arises because the $^{128}Xe$ is itself produced in the irradiation). Taking $\phi = 1.3 \times 10^{19}$ $cm^{-2}$ (Table 1) and an effective combined thermal and epithermal $\sigma = 0.8$ barns, the ratio of excess $^{129}Xe$ to $^{128}Xe$ is only $5 \times 10^{-6}$. Thus, neutron capture by $^{128}Xe$ also appears insufficient to account for the observations.

Independently of these quantitative evaluations of potential artifacts, both would produce a linear relation between $^{129}Xe$ and $^{128}Xe$ but not change the value of the extrapolated trapped $^{129}Xe/^{130}Xe$.

To further clarify this problem we analyzed Xe in an *unirradiated* sample of ALH-78113 (Table 4). In the unirradiated sample the observed $^{129}Xe/^{130}Xe = 8.16 \pm 0.09$ is definitely higher than the air or AVCC values and also higher than the trapped value of $7.16 \pm 0.06$ (Table 6) inferred from the irradiated sample but essentially identical to the total value $(7.96 \pm 0.09)$ for the irradiated sample. We conclude that ALH-78113 definitely has excess $^{129}Xe^*$ and that while some of it is trapped some of it remains *in situ* and correlates with $^{128}Xe^*$.

The very low correlation slope observed for ALH-78113, and the corresponding age (Table 6), is an extreme value not previously observed in I-Xe analysis and is therefore to be viewed with suspicion. Nevertheless, by the arguments above the potential artifacts considered cannot account for the observations so the age assignment tentatively must be considered real.

Assuming the absolute age of Bjurbole to be around 4.50 AE, the corresponding absolute age of ALH-78113 is 4.29 AE. While such an age has not previously been observed by the I-Xe method, it is not *a priori* unprecedented or even implausible,

since there are numerous results by other techniques which give "ages" of various kinds for *nonchondritic* meteorites which are 100 Ma and more later than the characteristic age of chondrite formation. The most relevant comparison is with an I-Xe analysis of the aubrite Bishopville (PODOSEK, 1970, 1972), which showed excess $^{128}$Xe* but essentially no detectable excess $^{129}$Xe*. Unfortunately the difficulty of making spallation $^{129}$Xe corrections for Bishopville makes setting an interesting limit on its I-Xe age impossible, but the best interpretation is that Bishopville formed clearly later than most chondrites.

All factors considered it appears that the aubrite ALH-78113 (and probably the aubrite Bishopville as well) has had rather a different history than other aubrites (*e.g.* Shallowater and Pena Blanca Spring: *cf.*, PODOSEK, 1970) whose I-Xe formations are essentially contemporaneous with chondrites.

The liklihood of terrestrial I contamination of Antarctic meteorites, and the effect of such contamination on I-Xe dating, will obviously require additional study, and we must reemphasize that pending such study the nominal conclusions reached for these two meteorites must be considered tentative. Thus, even for Y-691 the I content is higher than other E chondrites and terrestrial contamination must be suspected. For Y-691 most of the $^{128}$Xe* is already released before the high-temperature correlation is established, and it can thus be argued that contamination, if it occurred, does not affect the chronological interpretation. This is not the case for ALH-78113, and if the high I content of this meteorite is indeed mostly terrestrial contamination, this contaminant I nevertheless correlates with indigenous $^{128}$Xe* (Fig. 5) and its distribution within the meteorite must therefore be rather similar to the distribution of indigenous I.

## Acknowledgments

We wish to thank Prof. T. NAGATA and Dr. K. YANAI of the National Institute of Polar Research for providing the samples. We appreciate the excellent cooperation of A. MEYER and the staff at the University of Misouri Research Reactor Facility and also appreciate the assistance of R. KOROTEV in analyzing the flux wires. We also thank F. E. KRAMER for technical assistance, also E. KOENIG and B. WILCOX for manuscript preparation, and T. KORNMEIER for the photography. This work was supported by NSF grant EAR-81-16361, NASA grant NAG9–55, and by the McDonnell Center for the Space Sciences.

## References

BERNATOWICZ, T. J., HOHENBERG, C. M., HUDSON, B. G., KENNEDY, B. M. and PODOSEK, F. A. (1978): Argon ages for Lunar breccias 14064 and 15405. Proc. Lunar Planet. Sci. Conf. 9th, 905–919.

CAFFEE, M. W., HOHENBERG, C. M., HORZ, F., HUDSON, B., KENNEDY, B. M., PODOSEK, F. A. and SWINDLE, T.D. (1982): Shock disturbance of the I-Xe system. Proc. Lunar Planet. Sci. Conf. 13th, Pt. 1, A318–A330 (J. Geophys. Res., **87**, Suppl.).

CRABB, J. and ANDERS, E. (1981): Noble gases in E-chondrites. Geochim. Cosmochim. Acta, **45**, 2443–2464.

DROZD, R. J. (1974): Krypton and xenon in Lunar and terrestrial samples. Washington University, St. Louis, Ph. D. dissertation.

HOHENBERG, C. M. and KENNEDY, B. M. (1981): I-Xe dating; Intercomparisons of neutron irradiations and reproducibility of the Bjurbole standard. Geochim. Cosmochim. Acta, **45**, 251–256.

HOHENBERG, C. M., HUDSON, B., KENNEDY, B. M. and PODOSEK, F. A. (1981a): Xenon spallation systematics in Angra dos Reis. Geochim. Cosmochim. Acta, **45**, 1909–1915.

HOHENBERG, C. M., HUDSON, B., KENNEDY, B. M. and PODOSEK, F. A. (1981b): Noble gas retention chronologies for the St. Séverin meteorite. Geochim. Cosmochim. Acta, **45**, 535–546.

HUDSON, G. B. (1981): Noble gas retention chronologies for the St. Séverin meteorite. Washington University, St. Louis, Ph. D. dissertation.

HUDSON, G. B., KENNEDY, B. M., PODOSEK, F. A. and HOHENBERG, C. M. (1983): The early solar system abundance of $^{244}$Pu as inferred from the St. Severin chondrite. submitted to J. Geophys. Res.

HUNEKE, J. C. and SMITH, S. P. (1976): The realities of recoil; $^{39}$Ar recoil out of small grains and anomalous age patterns in $^{39}$Ar-$^{40}$Ar dating. Proc. Lunar Sci. Conf. 7th, 1987–2008.

KEIL, K. (1968): Mineralogical and chemical relationships among enstatite chondrites. J. Geophys. Res., **73**, 6945–6976.

KENNEDY, B. M. (1981): Potassium-Argon and iodine-xenon gas retention ages of enstatite chondrite meteorites. Washington University, St. Louis, Ph. D. dissertation.

KENNEDY, B. M. and PODOSEK, F. A. (1978): Iodine-xenon chronology of enstatite meteorites. U. S. Geol. Surv., Open File Rep. **78-701**, 211–213.

MASON, B. (1981): Antarct. Meteorite Newsl., **4** (1), 91.

NIEMEYER, S. (1979): I-Xe dating of silicate and troilite from IAB iron meteorites. Geochim. Cosmochim. Acta, **43**, 843–860.

OKADA, A. (1975): Petrological studies of the Yamato meteorites. Part 1. Mineralogy of the Yamato meteorites. Mem. Natl Inst. Polar Res., Spec. Issue, **5**, 14–66.

OKADA, A., YAGI, K. and SHIMA, M. (1975): Petrological studies of the Yamato meteorites. Part 2. Petrology of the Yamato meteorites. Mem. Natl Inst. Polar Res., Spec. Issue, **5**, 67–82.

PODOSEK, F. A. (1970): Dating of meteorites by the high-temperature release of iodine-correlated $Xe^{129}$. Geochim. Cosmochim. Acta, **34**, 341–365.

PODESEK, F. A. (1972): Gas retention chronology of Petersburg and other meteorites. Geochim. Cosmochim. Acta, **36**, 755–772.

SHIMA, M., SHIMA, M. and HINTENBERGER, H. (1973): Chemical composition and rare gas content of four new detected Antarctic meteorites. Earth Planet. Sci. Lett., **19**, 246–249.

SHIMIZU, H. and MASUDA, A. (1981): REE, Ba, Sr and Rb abundance in some unique Antarctic achondrites. Mem. Natl Inst. Polar Res., Spec. Issue, **20**, 211–220.

STEIGER, R. H. and JAGER, E. (1977): Subcommission on geochronology; Convention on the use of decay constants in geo- and cosmochronology. Earth Planet. Sci. Lett., **36**, 359–362.

TURNER, G., HUNEKE, J. C., PODOSEK, F. A. and WASSERBURG, G. J. (1971): $^{40}$Ar-$^{39}$Ar ages and cosmic ray exposure ages of Apollo 14 samples. Earth Planet. Sci. Lett., **12**, 19–35.

TURNER, G., ENRIGHT, M. C. and CADOGAN, P. H. (1978): The early history of chondrite parent bodies inferred from $^{40}$Ar-$^{39}$Ar ages. Proc. Lunar Planet. Sci. Conf. 9th, 989–1025.

VAN SCHMUS, W. R. and WOOD, J. A. (1967): A chemical-petrologic classification for the chondritic meteorites. Geochim. Cosmochim. Acta, **31**, 747–765.

WATTERS, T.R. and PRINZ, M. (1979): Aubrites; Their origin and relationship to enstatite chondrites. Proc. Lunar Planet. Sci. Conf. 10th, 1073–1093.

*(Received June 19, 1983; Revised manuscript received September 26, 1983)*